Direct electrodeposition of aluminium nano-rods

Emilie Perre [a,b], Leif Nyholm [a], Torbjörn Gustafsson [a], Pierre-Louis Taberna [b], Patrice Simon [b], Kristina Edström [a,*]

[a] Department of Materials Chemistry, The Ångström Advanced Battery Centre, Uppsala University, Box 538, SE-751 21 Uppsala, Sweden
[b] Université Paul Sabatier, CIRIMAT UMR CNRS 5085, 118 rte de Narbonne, 31062 Toulouse Cedex 9, France

A B S T R A C T

Electrodeposition of aluminium within an alumina nano-structured template, for use as high surface area current collectors in Li-ion microbatteries, was investigated. The aluminium electrodeposition was carried out in the ionic liquid 1-ethyl-3-methylimidazolium chloride:aluminium chloride (1:2 ratio). First the aluminium electrodeposition process was confirmed by combined cyclic voltammetry and electrochemical quartz crystal microbalance measurements. Then, aluminium was electrodeposited under pulsed-potential conditions within ordered alumina membranes. A careful removal of the alumina template unveiled free standing arrays of aluminium nano-rods. The nano-columns shape and dimensions are directly related to the template dimensions. To our knowledge, this is the first time that direct electrodeposition of aluminium nano-pillars onto an aluminium substrate is reported.

Keywords:
Aluminium
Electrodeposition
Ionic liquid
Three-dimensional microbattery

1. Introduction

New and highly promising micro/nano electromechanical systems (MEMS/NEMS) are now developed with refined manufacturing-techniques. Such devices require integrated batteries in order to be efficiently powered. Long et al. [1] have discussed the feasibility of such batteries and showed that three-dimensional nano-structured Li-ion microbatteries could satisfy the power expectations of certain MEMS such as smart dust motes. There are a number of different designs for 3D microbatteries that have been proposed and studied [1–3]. Taberna et al. [3] have successfully assembled a half-cell with a current collector consisting of free standing copper pillars coated by Fe_3O_4 as anode material. Such configuration allowed reaching a power density up to six times larger than the values measured on identically prepared planar batteries. Integrating current collectors in the 3D design allows suppressing the length limitation of the nano-rods (thus capacity limitation) due to electron conduction. On the cathode side, the generally high voltage ($\sim$4 V) in a Li-ion battery requires a corrosion resistant current collector and so far the only possible cheap pure metal is aluminium. To date, even though the synthesis of aluminium arrays has been presented [4–6], there is no report in the literature showing the direct electrodeposition of aluminium nano-rods on an aluminium foil.

In this study, we report the mechanism for electrodeposition of aluminium on a planar aluminium substrate and how this can be extended to the deposition of free standing aluminium nano-structured rods using porous alumina as template with the goal of producing current collectors for the positive side in 3D microbatteries.

2. Experimental

All the chemicals and electrochemical measurements were handled and carried out under inert atmosphere in an argon filled glove-box (O_2, H_2O < 2 ppm). 1-Ethyl-3-methylimidazolium chloride (98.5%, Fluka) and aluminium chloride (anhydrous powder, 99.99%, Sigma–Aldrich) were used as received without any further purification. The acidic ionic liquid (2:1 molar ratio of $AlCl_3$/[EMIm]Cl) was prepared by slow addition of $AlCl_3$ in [EMIm]Cl under continuous stirring. The reaction between the two compounds is highly exothermic, therefore care must be taken to avoid ionic liquid decomposition.

The electrochemical measurements were performed using a three electrodes cell connected to a potentiostat/galvanostat Autolab PGSTAT30. Working and counter electrodes were aluminium foils (99%, Goodfellow). The reference electrode was an aluminium wire of 1 mm diameter (99.999%, Goodfellow) directly immersed in the ionic liquid.

For electrochemical quartz crystal microbalance (EQCM) measurements, the working electrode was a gold coated 9 MHz AT-cut quartz crystal (Seiko EG&G model QA-A9M-Au-50) of 0.196 cm^{-2} area. In order to expose only one side to the electrodepositing solution, the crystal was mounted into a Teflon cell holder. Data were recorded with a quartz crystal analyser (SEIKO EG&G model QCA 922) and the WinEchem software (EG&G). The gate

Corresponding author.
E-mail address: Kristina.Edstrom@mkem.uu.se (K. Edström).

time was set to 0.1 s. Under the experimental conditions employed a frequency change of 1 Hz corresponded to a mass variation of 1.068 ng.

Prior to any use, the aluminium electrodes were degreased in acetone and mechanically polished with emery paper.

To obtain aluminium nano-pillars, pulsed-potential electrodeposition was performed through a nano-structured alumina template pressed in between the working electrode and a thick glass fibre separator filled with electrolyte. The cell corresponds to the setup already described [3]. Working and counter electrodes were both 1.0 × 1.0 cm aluminium sheets thus avoiding electrolyte consumption during the electrodeposition.

Following each electrodeposition, the obtained samples were washed in an acetonitrile solution.

Free standing aluminium nanopillars were obtained by dissolving the alumina template, outside the glove-box, in an aqueous solution of CrO_3 (1.8 wt.%) and H_3PO_4 (6 wt.%) [7] followed by rinsing in acetone.

All deposits were observed by scanning electron microscopy (LEO 1550).

3. Results and discussion

Many groups have reported aluminium electrodeposition on a wide range of substrates (Pt, Au, W, glassy C, Al, Fe, Cu) using different kinds of chloro-aluminate ionic liquids [8–15]. We have used the combination of 1-ethyl-3-methylimmidazoilum chloride ([EMIm]Cl) and aluminium chloride ($AlCl_3$) salts (2:1 ratio) where metallic aluminium is obtained through reduction of the $Al_2Cl_7^-$ anion. However, electrodeposition of aluminium nano-rods on aluminium substrate within an ordered alumina membrane could not be directly made by simply transposing the setup previously used for Cu deposit [3]. We thus studied the reduction of aluminium electrodeposition onto planar substrate.

3.1. Deposition of aluminium on planar substrate

Cyclic voltammetry measurements were performed at different scan rates on aluminium electrodes in highly stirred solutions (1200 rpm). Fig. 1 shows a typical cyclic voltammogram recorded at 20 mV s^{-1}.

The shape of the cyclic voltammograms obtained with an aluminium electrode corresponds well to the results previously presented by Jiang et al. [15]. The observed cathodic branch is due to aluminium electrodeposition from $Al_2Cl_7^-$, whereas the anodic shoulder corresponds to the oxidation of the deposited aluminium since electrolyte oxidation at such low anodic potential [16] should not be expected.

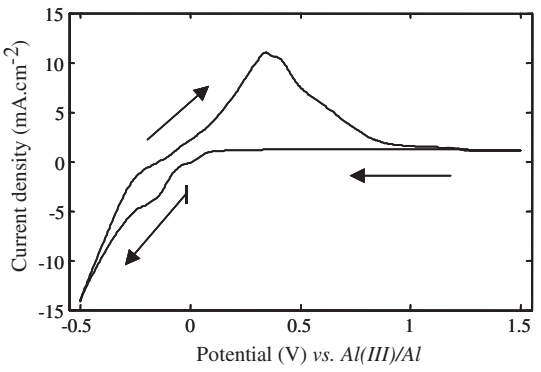

Fig. 1. Typical cyclic voltammogram recorded at 20 mV s^{-1} on Al working electrode in 2:1 ratio $AlCl_3$:[EMIm]Cl at 60 °C.

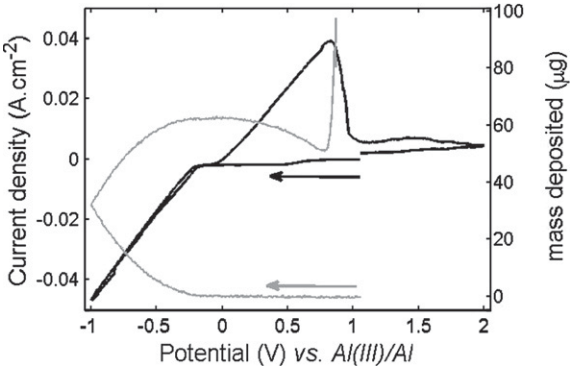

Fig. 2. Cyclic voltammogram at 10 mV s^{-1} combined with EQCM results both recorded simultaneously on Au-coated quartz crystal working electrode in 2:1 ratio $AlCl_3$:[EMIm]Cl at 60 °C.

Those results were confirmed using electrochemical quartz crystal microbalance while running a cyclic voltammetry measurement onto the gold-coated quartz crystal. The current density measured by CV and the mass variation measured by EQCM are plotted vs. the corresponding scanned potential (Fig. 2).

During the cathodic scan, there is a linear relationship between the mass and the charge. The slope is directly proportional to the molar weight of the deposit. Considering a three-electron process of $Al_2Cl_7^-$ reduction to Al, the calculated molar weight is 22.96 g mol^{-1}. Taking into account the aluminium molar weight (26.98 g mol^{-1}), the Faradic efficiency of the deposition process is 85%.

While subsequently scanning until 2 V vs. Al(III)/Al, one notes a sudden mass increase at 0.8 V that corresponds to a sharp decrease of the anodic current. This is ascribed to the precipitation of a solid layer on the aluminium electrode surface.

3.2. Growing aluminium nano-rods

The main objective of growing three-dimensional current collectors is to increase the active surface area while maintaining the small foot-print area of the battery. Using porous and ordered alumina as template for the electrodeposition of aluminium is advantageous since it is easy to manufacture membranes with different pore diameters (pd) and interpore distances (ip) [17,18]. Considering that the three dimensional current collectors have been electrodeposited in a perfectly well-organised alumina template, one can model a 3D nano-structured electrode and compare its expected performance with a thin-film electrode (Fig. 3). The area gain (AG) compared to a flat current collector can be defined by the following formula (1):

$$\mathrm{AG} = 1 + \frac{\pi \cdot \mathrm{pd} \cdot h}{\mathrm{ip}^2 \cdot \sin\theta}, \tag{1}$$

where h is corresponding to the height of the aluminium columns directly linked to the overall electrodeposition process time. The total capacity of the electrode was calculated considering the standard active material $LiCoO_2$ deposited onto a 250 nm thick aluminium current collector. The thickness of the deposited active material was set to 20 nm and the capacity was evaluated for different 3D aluminium current collector characteristics (height of pillars and interpore distance). From such basic considerations, the electrode capacity of a 3D nano-structure can be compared to that of a flat 2D batteries (Fig. 3). As an example; if considering a layer of $LiCoO_2$ deposited onto a 3D current collector having 5 µm high pillars and a surface area 20 times larger than that of a flat current collector, the calculated capacity per g of electrode is three times larger

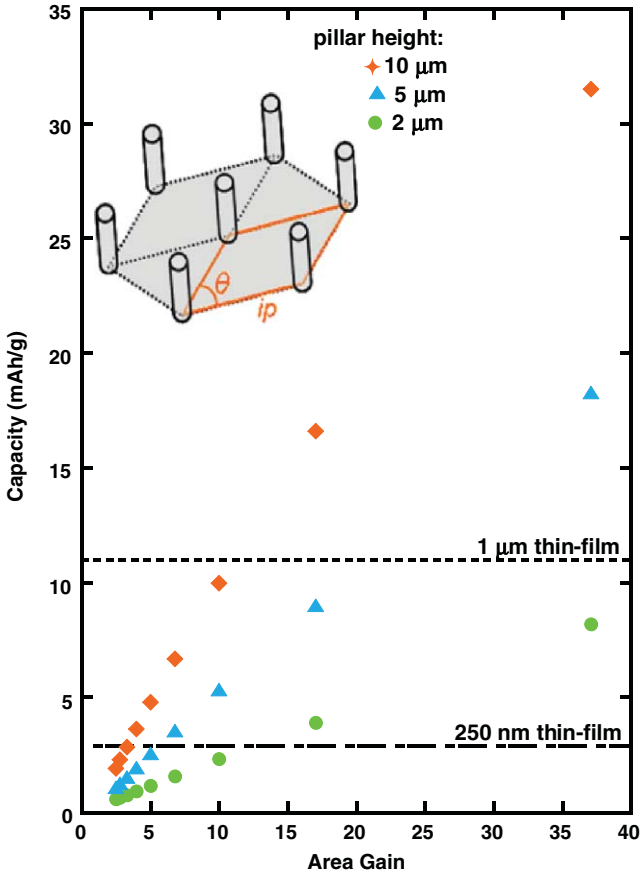

Fig. 3. Schematic representation of Al nanopillars grown in a perfectly well-organised alumina template is shown at the top left. Simulations of capacity per area gain have been made for a $LiCoO_2$ electrode material for a flat aluminium substrate (dashed lines where the $LiCoO_2$-layer is 250 nm or 1 µm) as well as for aluminium nano-pillars of different heights: 2 µm (green), 5 µm (blue) and 10 µm (red), respectively. In the simulation different interpore distances (ip) were considered for nano-rods with a width of 50 nm.

than the capacity for a 250 nm thin film of the same material deposited on the flat substrate. Simulations of how the length of the pillars and the interpillar distance influence the AG and the electrode capacity are shown in Fig. 3.

3.2.1. Electrochemical deposition of aluminium nano-rod

As the electrolyte is trapped in a very confined space, one could not expect a good renewal of it at the surface of the working electrode during the aluminium deposition especially since no forced convection could be applied within this particular cell. Therefore different potential steps were applied in order to obtain satisfactory aluminium deposition. Ideally one step should act as a deposition step where most of the aluminium-containing anion should be reduced while the other should operate as a "relaxation" step during which electroactive species are allowed to diffuse to the working electrode surface.

According to the cyclic voltammogram (Fig. 1) recorded previously in the "open-cell", aluminium deposition is taking place when the applied potential is moved to potentials more negative than −55 mV and the current is proportionally increasing. The potential steps have thus been varied from −0.6 to 0.1 V. The best deposition results were obtained when a potential of −0.4 to −0.3 V was first applied for 50 ms followed by a second step to −0.1 V for 200 ms. An experiment for 1 h was enough for the growth of 10 µm long aluminium columns. Fig. 4 shows the typical current response observed during the electrodeposition process for one cycle: the potential was fixed at −0.4 V for 50 ms and then

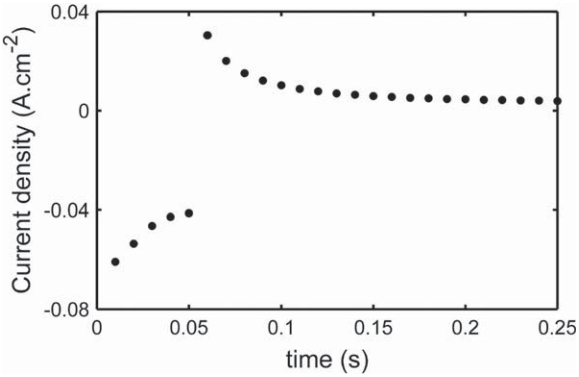

Fig. 4. Aluminium electrodeposition within alumina template, current response for one cycle: −0.4 V for 50 ms and −0.1 V for 200 ms.

stepped to −0.1 V for 200 ms. During the first step, aluminium was electrodeposited through the template, while during the second step the current measured was anodic. Measuring, for the same potential, different current values than the ones presented in the cyclic voltammetry (Fig. 1) is not unexpected since the electrodeposition cell configuration and hence also the iR drop totally different. A part of the deposited aluminium was stripped away, thus leading to a high concentration of active species at the electrode surface. Therefore during the subsequent step, electrodeposition was less affected by mass transport limitations.

Selection of the potential steps was a critical step. Indeed, working at higher cathodic potentials during the first step led to the formation of coatings with less homogeneous and less adherent nanopillars since the limitation due to diffusion was reached faster. Applying more cathodic potential during the second step also resulted in poor aluminium deposition, since when the potential was shifted back for the deposition, the aluminium reduction was still limited by the rate of diffusion. Of course, the potential should not be too anodic since then all the previously deposited aluminium will be removed.

3.2.2. Free standing aluminium nano-rods

We show that aluminium was successfully electrodeposited as nano-rods within ordered alumina templates under pulsed-potential conditions. Applying during 1 h, potential pulses of −0.4 V for 50 ms and −0.1 V for 200 ms, and afterwards dissolving the template led to an array of free standing aluminium columns, as shown in Fig. 5. The height of the aluminium columns is depending on the charge passed during the electrodeposition step, provided that the alumina membrane was well-impregnated with the ionic liquid prior to the electrodeposition. The morphology of the obtained pillars is entirely dependent on the alumina template used. The aluminium once deposited is completely filling the aluminium oxide pores. However, the template used has not a perfect ordering and displays defects. So once the template is removed, all the defects observed in the template are also visible among the aluminium pillars. This was particularly obvious when commercial membranes were used, as is shown in Fig. 5.

Care had to be taken during the alumina membrane removal to avoid any aluminium-pillar dissolution. A common procedure to remove a nano-porous alumina membrane is to use concentrated NaOH solution. In our experiment, this solution was reacting too strongly with the deposited aluminium. Instead the templates were removed by dipping the samples in a solution of 1.8 wt.% CrO_3 and 6 wt.% H_3PO_4 for 10 h. This solution is typically used during the two stepped-anodisation preparation of home-made alumina templates where the alumina formed after the first anodisation is removed from the aluminium substrate without destroying the texture created by the first anodisation step [7].

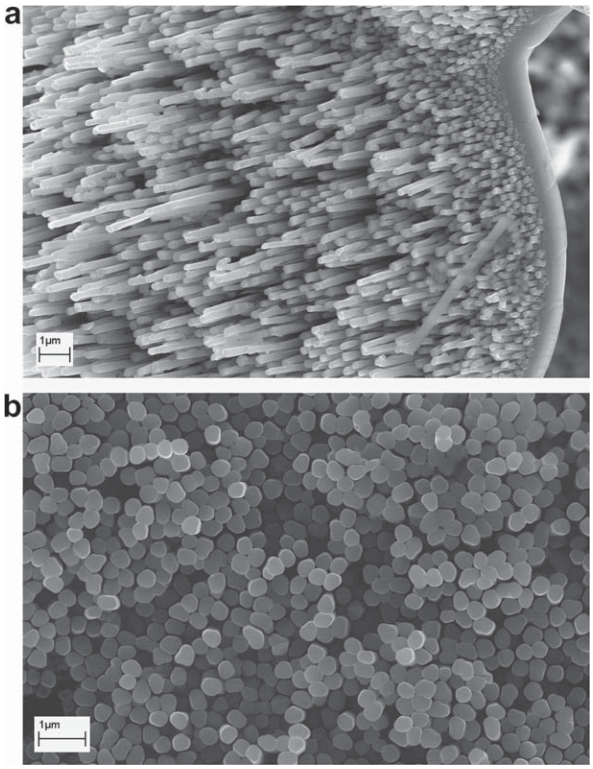

Fig. 5. Scanning electron micrographs of electrodeposited aluminium columns grown within different alumina templates (a) oblique view of an array of 200 nm diameter nanopillars; (b) top view of an array of 300 nm diameter nanopillars.

4. Conclusions

We show that it is possible to electrodeposit aluminium nanopillars of controlled size by the use of nano-porous alumina template membranes. Aluminium has been electrodeposited based on the reduction of $Al_2Cl_7^-$ in 1-ethyl-3-methylimidazolium chloride:aluminium chloride (1:2) ionic liquid. Potential steps with durations of a few milliseconds were applied periodically in order to get homogeneous deposits within the alumina pores. The template was finally dissolved, leading to arrays of free standing aluminium pillars, which will be used as a high surface area cathode current collector for microbatteries.

Acknowledgements

The authors would like to thank the European Commission for funding this work achieved in the frame of the ALISTORE Network of Excellence (FP6 programme) and the Swedish Research Council (VR).

References

[1] J.W. Long, B. Dunn, D.R. Rolison, H.S. White, Chem. Rev. 104 (2004) 4463.
[2] D. Golodnitsky, M. Nathan, V. Yufit, E. Strauss, K. Freedman, L. Burstein, A. Gladkich, E. Peled, Solid State Ionics 177 (2006) 2811.
[3] P.L. Taberna, S. Mitra, P. Poizot, P. Simon, J.M. Tarascon, Nature Mater. 5 (2006) 567.
[4] Y.T. Pang, G.W. Meng, L.D. Zhang, W.J. Shan, C. Zhang, X.Y. Gao, A.W. Zhao, Solid State Sci. 5 (2003) 1063.
[5] C. Li, W. Ji, J. Chen, Z. Tao, Chem. Mater. 19 (2007) 5812.
[6] M. Kokonou, C. Rebholz, K.P. Giannakopoulos, C.C. Doumanidis, Nanotechnology 18 (2007) 495604.
[7] H. Masuda, M. Satoh, Jpn. J. Appl. Phys. 35 (1996) L126.
[8] Y. Zaho, T.J. VanderNoot, Electrochim. Acta 42 (1997) 3.
[9] P.K. Lai, M.J. Skyllas-Kazacos, Electroanal. Chem. 248 (1988) 431.
[10] R.T. Carlin, W. Crawford, M.J. Bersch, Electrochem. Soc. 139 (1992) 2720.
[11] Y. Zaho, T.J. VanderNoot, Electrochim. Acta 42 (1997) 1639.
[12] A.P. Abbott, C.A. Eardley, N.R.S. Farley, G.A. Griffith, A.J. Pratt, Appl. Electrochem. 31 (2001) 1345.
[13] F. Endres, M. Bukowski, R. Hempelmann, H. Natter, Angew. Chem. Int. Ed. 42 (2003) 3428.
[14] V. Kamavaram, D. Mantha, R.G.J. Reddy, Min. Met. 39 (2003) 43.
[15] T. Jiang, M.J. Chollier Brym, G. Dubé, A. Lasia, G.M. Brisard, Surf. Coat. Technol. 201 (2006) 1.
[16] M. Lipsztajn, R.A. Osteryoung, J. Electrochem. Soc. 130 (1983) 1968.
[17] A.P. Li, F. Müller, A. Birner, K. Nielsch, U.J. Gösele, Appl. Phys. 84 (1998) 6023.
[18] W. Lee, R. Ji, U. Gösele, K. Nielsch, Nature 5 (2006) 741.